DOE/FETC-99/1083

Flow Visualization Studies in the Novacor Left Ventricular Assist System CRADA PC91-002, Final Report

Harvey S. Borovetz
Frank Shaffer
Richard Schaub
Laura Lund
John Woodard

no date
(Submitted January 1999)

U.S. Department of Energy
Federal Energy Technology Center
P.O. Box 10940
626 Cochrans Mill Road
Pittsburgh, PA 15236-0940

and
University of Pittsburgh
350 Thackery Hall
Pittsburgh, PA 15260-4020

Disclaimer

Pc 91-002

Flow Visualization Studies in the Novacor Left Ventricular Assist System

Harvey S. Borovetz[1], Frank Shaffer[2], Richard Schaub[1], Laura Lund[1] and John Woodard[3]

Abstract

This paper discusses a series of experiments to visualize and measure flow fields in the Novacor left ventricular assist system (LVAS). The experiments utilize a multiple exposure, optical imaging technique called fluorescent image tracking velocimetry (FITV) to track the motion of small, neutrally-buoyant particles in a flowing fluid.

Introduction

Since 1988, the Novacor LVAS (Portner et al, 1989) has sustained 27 cardiac transplant candidates at the University of Pittsburgh Presbyterian Hospital. Particularly impressive is the fact that of the patients who received a donor heart (18/27), all were discharged home well (Kormos et al, 1991). Nonetheless complex problems remain to be solved if the Novacor LVAS and other implantable blood pumps are to achieve widespread clinical use (Didisheim et al, 1989).

The motivation for this work is to further understand the dynamics of blood flow in the Novacor LVAS. In this project we use state-of-the art flow diagnostic tools to analyze flow fields around the pericardial valves of the Novacor LVAS.

[1]Department of Surgery, University of Pittsburgh, Pittsburgh, PA 15261
[2]U.S. Department of Energy, P.O. Box 10940, Pittsburgh, PA 15236
[3]Novacor Division, Baxter Healthcare Corp, 7799 Pardee Lane, Oakland CA 94261

FITV Methodology

Fluid dynamic measurements are done with a technique called fluorescent image tracking velocimetry (FITV). FITV enables measurements to be made very close to biomaterial surfaces. Here a fluid is seeded with particles that follow the fluid flow – that is, neutrally-buoyant particles with low Stokes numbers and sizes much smaller than the length scales of the flow. A pulsed laser illuminates the seeded flow field at controlled intervals. The displacement of particles between laser pulses produces a velocity vector map of flow field. From this, other important parameters, such as shear stress and particle residence time, can be directly calculated.

FITV involves seeding the fluid with particles which fluoresce when excited with light of an appropriate wavelength. An important property of the fluorescent dye is its Stokes shift – the difference in excitation and emission wavelengths. Thus, the light from the seeded particles consists of both scattered light at the excitation wavelength, δ_1, and fluoresced light at a different wavelength (mean fluorescent emission, δ_2). Adjacent to solid boundaries in the Novacor LVAS, the light scattered by the flow boundary is at the same wavelength, δ_1, as the excitation light. Almost always, the intensity of the light scattering by the solid boundary is much stronger than that from the seeded particles. The result is a low signal-to-noise (S/N) ratio for particles near the flow boundary.

The S/N ratio is increased dramatically by placing an excitation filter in front of the imaging camera. The excitation filter occludes the light scattered by the flow boundary at δ_1 – the camera sees only the fluorescent light emitted by particles at δ_2. This approach has provided excellent S/N ratios of particles adjacent to the pericardial valves in the Novacor LVAS.

Cardiac Simulation Flow Loop

For this study it is essential to acquire the FITV data under realistic patient hemodynamic conditions. To this end, a cardiac simulation system is interfaced with the Novacor LVAS as shown in Figure 1. This allows simulation of the flow conditions (pump stroke volumes, frequencies, rate of filling and pump outputs) monitored in Novacor LVAS patients at the University of Pittsburgh.

A Novacor LVAS was manufactured from transparent materials to provide optical access for FITV. A transparent blood analog fluid is also used (42% by wt. aqueous spectrophotometric-grade glycerin). The blood analog fluid is seeded with "red" fluorescent particles manufactured by

Duke Scientific Corporation (Duke Scientific Corporation, Palo Alto, CA). The particles are neutrally buoyant and their size is 30 ± 2 microns.

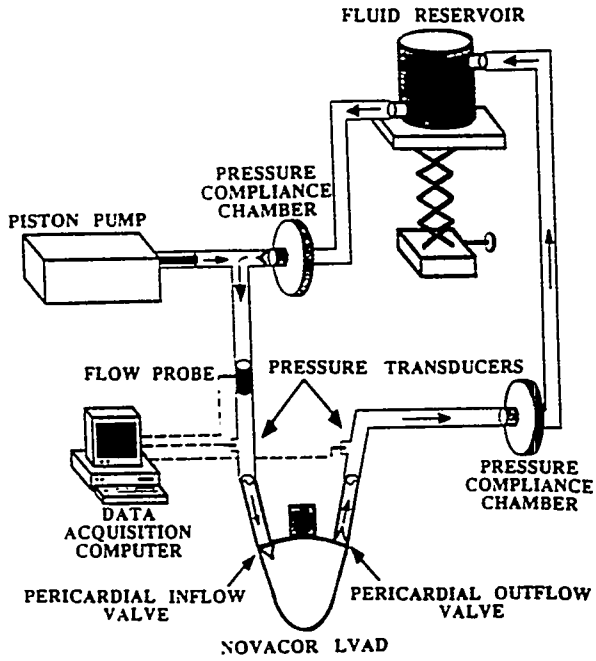

Figure 1. Cardiac simulation flow loop

Results and Discussion

The flow conditions for FITV measurements simulate the full range of clinical conditions observed for cardiac transplant candidates at the University of Pittsburgh: pump rates extend between 60 to 120 beats/minute with fill volumes ranging from 25 to 60 cc.

Figures 2 displays a typical FITV image acquired at a pulse frequency of 222 Hz. This image corresponds to the time in the pump cycle when the valve leaflets are stationary and the particle velocities adjacent to the pericardial valve are low. During the opening and closing phases of the valve leaflets, the velocities are elevated, suggesting an important contribution of the leaflet motion to "valve washing" and avoidance of areas of stasis.

By providing high resolution, quality images of the flow fields adjacent to the pump inflow and outflow valves (Figure 2), the present series of experiments yields new insight regarding Novacor LVAS fluid mechanics under realistic (clinical) conditions. For example, we have

documented the marked variation of the flow fields adjacent to the pericardial valve as a function of time (systole, diastole, etc) during the LVAS pumping cycle. Preliminary quantitative analyses of these images, which were obtained for an LVAS pumping rate of 100 beats/minute, indicate that the flow speed near the valve surface can vary by a factor of 50 during the LVAS pump cycle. Other images (not shown) demonstrate conclusively that both the volume rate of pump filling (dV/dt) and LVAS stroke volume profoundly influence the flow fields around the inflow and outflow valves. Our ongoing FITV studies are aimed at further exploring these and other hemodynamic variables which may be relevant to the clinical management of Novacor LVAS recipients.

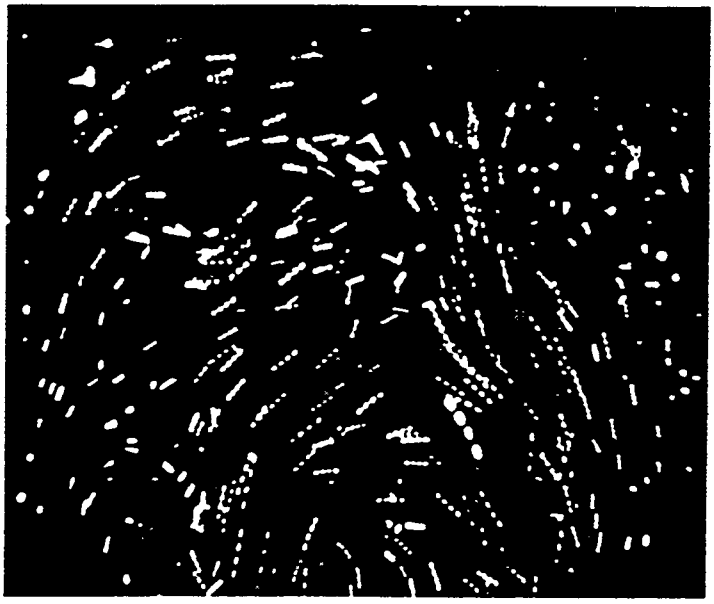

Figure 2. FITV derived flow pattern in the Novacor LVAS.

References

Didisheim P, Olsen DB, Farrar DJ et al, "Infections and Thromboembolism with Implantable Cardiovascular Devices" Transactions of the American Society for Artificial Internal Organs 1989; Vol 35, pp. 54-70.

Kormos RL, Borovetz HS, Armitage JM et al, "Evolving Experience with Mechanical Circulatory Support" Annals of Surgery 1991; Vol 214, pp. 471-477.

Portner PM, Oyer PE, Pennington DG et al, "Implantable Electrical Left Ventricular Systems: Bridge to Transplantation and to the Future" Annals of Thoracic Surgery 1989; Vol 47, pp. 142-150.

SLIDE FORUM 10

CIRCULATORY ASSIST/NEW DESIGNS

Development of an Axial Flow Blood Pump LVAS

KENNETH C. BUTLER,* TIM R. MAHER,* HARVEY S. BOROVETZ,† ROBERT L. KORMOS,† JAMES F. ANTAKI,† MARINA KAMENEVA,† BARTLEY P. GRIFFITH,† TONY ZERBE,† AND FRANK D. SCHAFFER‡

Nimbus, Inc., (Rancho Cordova, CA) and the University of Pittsburgh (Pittsburgh, PA) are collaborating to develop an implantable rotary blood pump that can be used as a left ventricular assist system (LVAS). The short-term goal of this project is to show that an LVAS based on this pump can operate safely and reliably during chronic implantations in animals. Work conducted to date includes *in vitro* testing of hydraulic performance, hemolysis, endurance demonstration, and flow visualization. Results indicate that the pump is capable of generating an output of up to 10 L/min at physiologic pressures. Associated electrical power to drive these pumps is in the range of 6–10 watts. One integrated pump was placed in a mock flow loop and operated continuously at a fixed speed (10,000 rpm), pressure (100 mmHg), and flow rate (6 L/min) for 90 days with no apparent difficulty. *In vitro* hemolysis test results have consistently ranged between 3–6 g of liberated hemoglobin/day, which is an acceptable range for chronic use. Two *in vivo* trials of 7 and 14 days were performed using calves, after which tests have been done using sheep as the animal model. Five short-term sheep experiments have been conducted with good results. Future studies will include implantations in sheep of 3 months duration. *ASAIO Journal* 1992; 38: M296–M300.

Practical considerations of mechanical circulatory support systems that offer the potential for chronic treatment of end-stage heart disease raise issues that extend beyond merely developing safe and effective devices. Three issues in particular are relevant to the effect of artificial heart technology on this nation's health care system[1]: 1) concern about the cost effectiveness of a mechanical circulatory support system (MCSS), that is, assuring that the aggregate increases in health care cost will be offset by improved patient outcomes; 2) concern that MCSSs will be used appropriately; and 3) concern relative to accessibility to MCSSs, for example, assuring that there will be equitable patient access to these life-saving therapies.

When these issues are translated to MCSS system features, it is apparent that several essential design requirements must be met.

First, an MCSS must possess the necessary flow performance, physiologic compatibility, durability, and reliability attributes currently expected of a chronic device. Second, MCSSs should be as small and simple as possible, be comparatively easy to implant and operate, and be anatomically compatible with the body habitus of both men and women. Finally, the cost of an MCSS should not be a barrier either to its development as a commercial product or to its clinical utilization by the medical community.

Nimbus and its development partner, the University of Pittsburgh's School of Medicine (UOP), believe that meeting these criteria will require new devices in addition to existing technology. Furthermore, the inherent small size and straightforward mechanical design associated with continuous flow pumps make these devices particularly attractive as future MCSSs. Consequently, Nimbus and the University have embarked on a joint venture to develop an implantable left ventricular assist system (LVAS) that uses an axial flow rotary pump to generate cardiac output.

Nimbus created the first miniature axial flow blood pump for the Hemopump, a 21 Fr. temporary LVAS that has undergone substantial clinical use in both the United States and Europe.[2–4] After developing the Hemopump, Nimbus began investigating a scaled-up version of the axial flow concept for chronic ventricular support.[5,6] The results of this investigation form the foundation for the project discussed below.

Methods

Axial Flow LVAS Description

The prototype for a chronically implanted axial flow LVAS, designated the AX-LVAS, is comprised of three major elements: 1) the integrated pump/motor, 2) an inflow and outflow cannulae set, and 3) the external controller and power

From *Nimbus, Inc., Rancho Cordova, California, the †University of Pittsburgh, Pittsburgh, Pennsylvania, and ‡U. S. Department of Energy, Pittsburgh Energy and Technology Center, Pittsburgh, Pennsylvania.

Reprint requests: Kenneth C. Butler, Nimbus Inc., 2945 Kilgore Rd., Rancho Cordova, CA 95670.

...ers. The current details of this evolving design are described below.

Blood Pump. **Figure 1** shows a photograph of the integrated motor/axial flow blood pump. This unit, which is fabricated from 347 stainless steel, weighs 62 g and displaces 82 mL. It has the capacity to pump 10 L/min of cardiac output at 120 mmHg aortic pressure and is fully capable of sustaining any physical activity chronic patients might undertake. **Figure 2** illustrates how the pump interfaces with the circulation through an inflow cannula cored into the left ventricular apex and an outflow cannula anastomosed to the ascending aorta.

The pump consists of a single axial stage rotor and matching stator integrated into the center of the drive motor. Journal bearings support the rotating assembly radially, and a hydrostatic face bearing provides axial thrust balance and a blood seal interface. Two cables connect the implanted unit to an external controller. One cable contains the electrical wires carrying current to the motor, whereas the second cable is a conduit that supplies a pressurized physiologic fluid to the interior of the pump for the bearing and blood seal lubrication. Approximately 15 mL/day of fluid is required to maintain seal patency (5% mixture of dextrose in water).

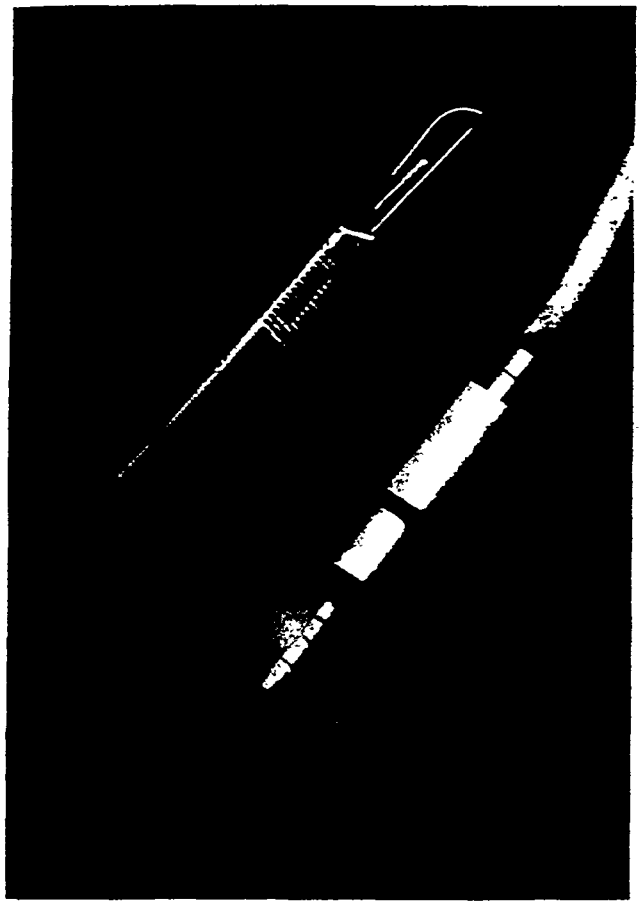

Figure 1. Implantable axial flow blood pump.

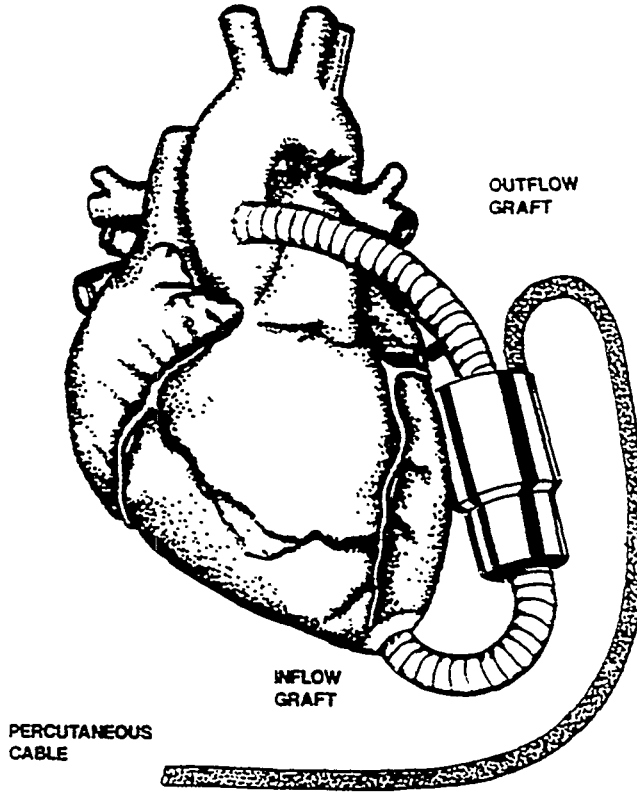

Figure 2. Axial flow left ventricular assist system anatomic placement.

Inflow and Outflow Cannulae. Inflow and outflow cannulae are configured for the left ventricular apex to ascending aorta connection. The inflow cannula is dip-cast from medical grade silicone rubber, and is a smooth-walled, wire reinforced conduit (10 mm i.d., ≈ 15 cm long). It is bonded to a stiff apical tube for penetration of the left ventricle, and heat formed to create the desired bend angle. The outflow cannula is a conventional expanded PTFE (Gore-Tex) graft.

External Controller

The controller has three basic functions. First, it provides primary electrical power and the control signals that energize the motor stator and vary the motor speed on demand. Second, it provides the purge fluid supply functions. Third, it displays diagnostic information: electrical power, motor speed, and purge pressure.

Flow Visualization Tests

Flow visualization techniques are being used to refine the flow geometry within the pump and inflow cannula. A laser-based particle tracking technique, termed fluorescent image tracking velocimetry (FITV), is being used to track the motion of neutrally buoyant, 30 μm diameter particles within the flow field.[7,8] An argon laser illuminates the seeded flow field with subsequent image processing providing frame-by-frame particle locations; summation of such successive

frames yields a vector map of the overall flow field. A special fixture is used, which has the pump hydraulic elements mounted in a transparent housing, driven by a flexible cable. The pump circulates a blood fluid analog containing the particles in a closed loop at specified flows and pressures. Figure 3 is a schematic illustration of the experimental set-up.

In Vivo Experiments

Initial *in vivo* studies of the AX-LVAS conducted by Nimbus consisted of two implantations in calves, one of 7 days and one of 14 days duration. The animal model currently used is the adult sheep. Thus far, sheep implantations have consisted of a series of short-term (≤1 week) studies. These tests are intended to 1) optimize the design of the blood pump and cannulae, 2) demonstrate hemodynamic capability of the implantable systems, and 3) characterize the interface reaction between the AX-LVAS and the host anatomy and physiology.

The pump is implanted through a sternotomy procedure. The inflow cannula is connected through an apical core made in the ventricle. The outflow graft is anastomosed in an end-to-side fashion to the aorta. After priming, pump operation is begun, and the implantation site is closed. After the animal recovers from anesthesia, it is placed in a specially designed stall, and thereafter is attended continuously by medical and veterinary staff. Routine monitoring includes an array of parameters for hematologic, biochemical, hemodynamic, and pump operating status.

Results

In Vitro Tests

Flow Performance. Pumps were tested *in vitro* over a range of rotating speeds and specified operating pressures. Volumetric flow rate was measured at each test condition, thereby generating a flow map. **Figure 4** displays one such map for the latest pump blade configuration using bovine blood as the flow medium at pressures that ranged from the

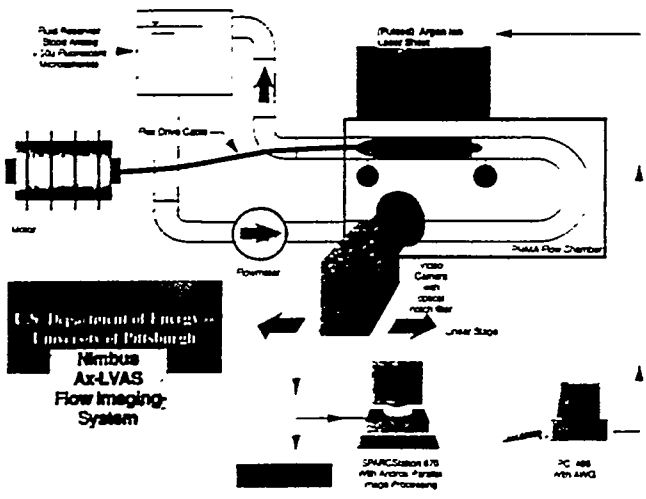

Figure 3. Flow visualization test schematic.

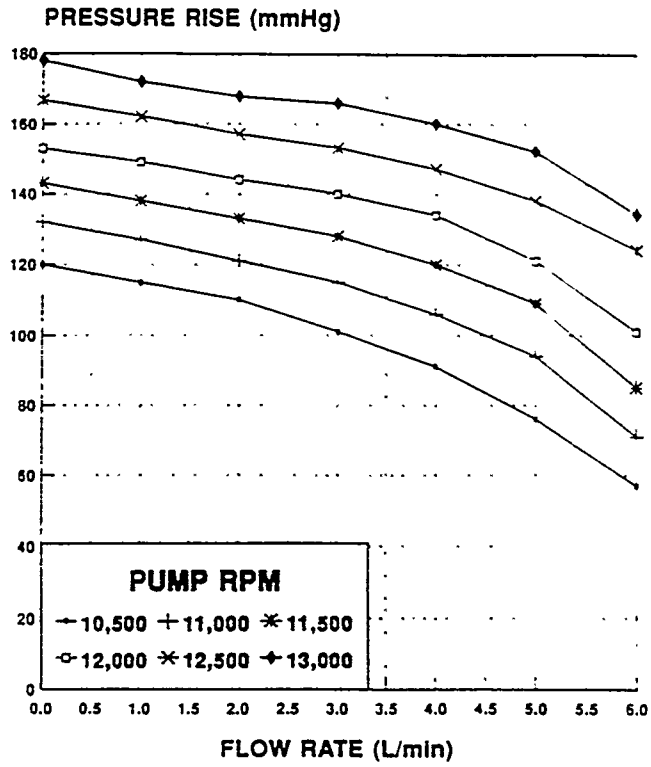

Figure 4. H-Q performance integrated pump S/N 003 in bovine blood.

flow 220 mmHg (shut-off condition) to 40 mmHg at the low end.

Hemolysis. Various blade configurations were tested for hemolysis generation using bovine blood. The amount of free hemoglobin liberated within a known volume of circulating blood is determined for specified intervals. The result is expressed as an average hemolysis index in grams per day. Results for one continuous test of the latest blade design are listed in **Table 1.** For reference, the Hemopump's bench mark level is 4 g/day. A value lower than 10 g/day is the generally accepted level for device related hemolysis (**Table 1**).

Endurance Demonstration. An integrated pump was placed in a flow loop containing normal saline and operated continuously at a fixed speed and pressure (6 L/min, 100 mmHg) for 91 days, the intended duration. Purge flow rate was maintained at an average value of 20 ml/day. During the test, the pump's operating parameters stayed within normal ranges.

Table 1. Axial Blood Pump *In Vitro* Hemolysis Test Results

Pressure (mmHg)	Flow (L/min)	Speed (rpm)	Hemolysis (gm/day)
100	5.0	11,000	4.0
120	5.0	12,000	4.0
140	5.0	13,600	5.9
100	7.0	12,000	3.5

Post-test inspection of the pump components showed that the bearing and seal surfaces experienced virtually no wear and thus were capable of much longer perfusion times. The most significant finding was the presence of corrosion on stainless steel components in static contact with the same, which is caused by crevice corrosion mechanisms and is an anticipated result of long-term exposure of stainless steel to saline. However, the degree of corrosion was such that the pump could have run considerably longer before structural degradation would have affected pump operation. This problem is being corrected by switching from the 347 stainless steel used in previous pumps to a 6 AL-4V titanium alloy.

Flow Visualization. These are on-going tests, and results are preliminary. The flow field has been mapped at discrete locations within the inflow cannula, at the entrance to the rotor, between adjacent rotor blades, at the rotor exit-stator entrance section, and at the stator exit. Examination of the flow streamline patterns suggests that the blade angles are properly oriented, and that no significant areas of recirculation or separation develop during normal operation of the pump. There does appear to be a relatively high velocity impact area in the pump's inducer section, and this is being studied further.

In Vivo Tests

Implantation Duration. Five sheep have been implanted with the AX-LVAS. Implantation times ranged from 12 to 72 hr. All cases were electively terminated, and the sheep were in no apparent discomfort at the time they were killed. No device related problems occurred.

Hematologic, Hemodynamic, and Biochemical Evaluation. After the initial postoperative period, pump speeds were maintained between 10,000 and 12,000 rpm. Pump outputs exceeded 6 L/min. Left ventricular decompression was verified by visual inspection before chest closure and thereafter by measurement of left atrial pressure. A diminished pulse pressure was routinely observed in these animals (e.g., from ≥30 mmHg pre-implantation to 10–20 mmHg at rpm ≥ 10,000). Arterial blood gases (pH, pO_2, and pCO_2) generally remained within normal limits. Consistent with the *in vitro* findings, the electrical power required by the system to generate this performance ranged between 7 and 10 watts.

Electrolyte concentrations, creatinine, BUN, total protein, and liver enzymes all remained at baseline (pre-implantation) norms. **Table 2** details the plasma free hemoglobin levels as a function of time and pump speed in one recent experiment. A slight rise in hemolysis at 24 hr was followed by a return toward baseline by 3 days after implantation. Other indices of blood rheology, including asymptotic Estimate Newtonian blood viscosity, plasma viscosity, and erythrocyte rigidity, did not change significantly from pre-implantation values. Average values for hematocrit ranged from 22% to 27% (**Table 2**).

Table 2. Axial Blood Pump *In Vivo* Hemolysis Test Results

Implant Time	Speed (rpm)	Plasma Hemoglobin (mg/dl)
Baseline	—	2.0
1 hour	11,200	4.5
8 hours	10,100	4.5
12 hours	10,100	7.0
24 hours	11,200	27.0
48 hours	11,400	27.5
72 hours	11,400	13.5

Necropsy. Focal renal emboli were observed in the first two sheep. After refinement of the design and fabrication of the cannulae, no renal or pulmonary emboli were documented. In several of the animals, examination of the cardiac chambers indicated ischemic injury near the insertion site of the inflow cannula, suggestive of decompression of the left ventricle around the cannulation site. Lung atelectasis was documented in one animal. No remarkable findings were noted for the liver or other organs. There has been no indication of tissue damage due to excessive device interface temperatures.

The pump flow passages have been found to be generally free of cellular debris. Microscopic deposits of debris have been noted at interface discontinuities along the blood seal and along the outer edges of the stator blades, both of which are normal findings. Predictably, there has been no trace of blood elements behind the seal.

Conclusions

Our results to date with the AX-LVAS support the assertion that this device can meet the essential requirements of a chronic MCSS. Compared with existing pulsatile devices its small size and simple nature address the need of ease of implantation and applicability to a broad patient population. These features also mean significantly lower costs, not only for the clinical product but for the program that will be required to obtain Food and Drug Administration approval of this Class III device. In addition, these features will lower the risk of development and qualification, which will also decrease costs.

Test results of integrated blood pump/motor units indicated that the fluid supported bearings and seal offer the potential for an exceedingly long operation life for the pump. In addition, the basic biocompatibility of the AX-LVAS has been verified by both *in vitro* and *in vivo* results. To be sure, further *in vivo* testing and *in vitro* reliability testing lie ahead to prove the capabilities of the AX-LVAS conclusively.

The key to the life potential of the AX-LVAS is use of the active purge fluid to lubricate the seal and bearings. Obviously, this approach complicates the design and use of this pump compared with one that does not require an external lubricating fluid. However, the Nimbus/UOP research team firmly believes that this complication can be addressed in the clinical setting, as well as in every day life situations of chronic patients. An important basis for this belief is the experience of the UOP team in the care of MCSS patients in non-hospital settings.[9]

The major reason to eliminate the purge requirement is that it is not compatible with a totally implanted MCSS. We

and others, are working on concepts that do not require lubrication with external fluid. However, these concepts are in the early development stage, and all are faced with a long and risky development course. This fact is illustrated by the dilemma associated with blood lubricated bearings, for which the only way to verify endurance capability is through long-term testing in coagulable blood: a very difficult and costly undertaking. In the long-term, implanted rotary pump LVASs that do not require percutaneous lines will surely be justified. In addition to the blood pump, these systems will require an implanted internal battery, a transcutaneous energy transmission system and its implanted coil, and an implanted miniature electronic controller. Significantly more complicated systems are involved, as are more extensive surgery and increased cost factors. Indeed, these complications represent a departure from our vision of what an ideal, widely used device should be.

In one sense, the percutaneous AX-LVAS can be viewed as an interim device, a necessary and important step toward development of totally implanted blood pump systems based on continuous flow technology. On the other hand, it may also be entirely suitable for some chronic patients, for whom the higher risks associated with percutaneous access may be offset by the lower cost and ease of implantation of the simpler system. The motivation for development of purge-less pumps will evolve as we move towards totally implantable LVASs. Meanwhile, there is much to be gained with this AX-LVAS approach, both in terms of potential clinical trials and the knowledge to be derived from the clinical use of continuous flow devices.

References

1. Hogness JR, VanAntwerp M (eds): *The Artificial Heart: Prototypes, Policies, and Patients*. Washington: National Academy Press, 1991.
2. Butler KC, Moise IC, Wampler RK: The Hemopump: a new cardiac prosthesis device. *IEEE Trans Biomed Eng* 37: 193–196, 1990.
3. Frazier OH, Nakatani T, Duncan JM, et al: Clinical experience with the Hemopump. *Trans Am Soc Artif Intern Organs* 35: 604–606, 1989.
4. Wampler RK, Frazier OH, Lansing AM, et al: Treatment of cardiogenic shock with the hemopump left ventricular assist device. *Ann Thorac Surg* 52: 506–513, 1991.
5. Butler KC, Wampler RK, Maher TR, et al: Demonstration and evaluation of an implantable axial flow blood pump. *Proceedings of the Cardiovascular Science and Technology Conference (CVSTII)*, Bethesda, Maryland, 1991, p. 183.
6. Butler KC, Wampler RK, Griffith BP, et al: Development of an implantable axial flow LVAS. *Proceedings of the International Workshop on Rotary Blood Pumps*, Vienna, Austria, 1991, pp. 148–153.
7. Schaffer F, Ekmann J: Development of pulsed laser velocimetry systems utilizing photoelectric image sensors. *American Institute of Aeronautics and Astronautics: 1st Fluid Dynamic Congress*, Cincinnati, OH, 1988, pp. 1944–1952.
8. Schaffer F, Mathur M, Woodard J, et al. Fluorescent image tracking velocimetry applied to the Novacor left ventricular assist device. *Proceedings of the American Society of Mechanical Engineers Fluids Engineering Conference*. Los Angeles CA, June 1992.
9. Kormos RL, Borovetz HS, Winowich S, Armitage JM, Griffith BP: Out-of-hospital facility for the Novacor bridge to transplant patient: the Pittsburgh Family House Experience. *Abstracts ASAIO* 20: 13, 1991.

FLUORESCENT IMAGE TRACKING VELOCIMETRY APPLIED TO THE NOVACOR LEFT VENTRICULAR ASSIST DEVICE

F. Shaffer and M. Mathur
U.S. Department of Energy
Pittsburgh Energy Technology Center
P.O. Box 10940, Pittsburgh, PA 15236

J. Woodard
Baxter Healthcare, Novacor Division
7799 Pardee Lane, Oakland, CA 94261

H. Borovetz, R. Schaub, J. Antaki, R. Kormos and B. Griffith
University of Pittsburgh, Department of Surgery
Pittsburgh, PA 15260

R. Srinivasan and R. Singh
Science Applications International Corporation
P.O. Box 10940, Pittsburgh, PA 15236

C. McCreary
Gilbert Commonwealth
P.O. Box 10940, Pittsburgh, PA 15236

ABSTRACT

This paper discusses a technique, and the associated experimental equipment, to visualize and measure flow fields near biomaterial surfaces. The technique is called fluorescent image tracking velocimetry (FITV). It is a multiple exposure, optical imaging technique to track the motion of small, neutrally-buoyant particles in a fluid flow field. The particles may be small enough to follow the fluid flow and to approach the size of actual blood cells (1-10 microns).

The main advantage of FITV is the ability to measure the motion of small particles close to — even touching — a biomaterial surface. The motivation for this study is to achieve mappings of flow fields close to biomaterial surfaces in a type of artificial heart assist pump, the Novacor Left Ventricular Assist System (LVAS). Such measurements are critical in the effort to optimize hemodynamic conditions (e.g., velocities, shear rates, cell residence times) within the LVAS.

1.0 INTRODUCTION

In its recently released report to the National Heart, Lung and Blood Institute (NHLBI), the Institute of Medicine, through its Council on Health Care Technology, estimated that between 35,000 and 70,000 Americans annually require either permanent circulatory assist devices or cardiac transplantation [1]. For these patients, the therapy of choice remains cardiac transplantation. However, the donor heart supply is severely limited (1,673 cardiac transplants were performed in the United States in 1989) and is expected to remain so into the foreseeable future [2]. Thus, development of circulatory assist devices is critical to the survival of most of these heart-failure patients.

For the last 25 years, much of the work to develop circulatory assist devices involved pulsatile pumps that mimic the pumping action of the natural heart. Impressive progress has been made in solving the complex problems associated with the safe delivery of blood to the systemic circulation. In fact, several systems are now successfully used to support terminal cardiac patients who await transplantation [3,4]. One such device (Figure 1), the Novacor left ventricular assist system (NLVAS), has been used to support more than 100 heart-failure patients awaiting transplantation. Periods of support range from one day to 370 days. Since 1988, the NLVAS has sustained 27 cardiac transplant candidates at the University of Pittsburgh's Presbyterian Hospital. Particularly impressive is the fact that all of the patients who received a donor heart (18/27) were discharged from the hospital in good physical condition [5].

In spite of these encouraging clinical results, complex problems remain to be solved if these devices are to achieve widespread use. Problems of infection, bleeding, end-organ dysfunction, and thromboembolism have been reported by the various clinical centers utilizing these devices [6].

The motivation for this work is to optimize the hemodynamics of the LVAS and thus minimize the chance of undesirable activation of the hemostatic system in contact with biomaterial surfaces. This activation is likely a strong function of patient-dependent factors and the choice of biomaterials, but fluid-dynamic properties of the device are also important. Although the conditions that cause activation are not yet well understood, it is believed that high shear rates, areas of flow stasis and generation of strong recirculation zones are undesirable within any blood contacting device. By understanding the flow characteristics of the LVAS, this work will have immediate benefits for LVAS patients in that optimum modes of LVAS operation may be chosen as a function of their hemodynamic status. We have chosen to study the areas around the prothetic valves in the LVAS in which flow characteristics are likely to be most critical.

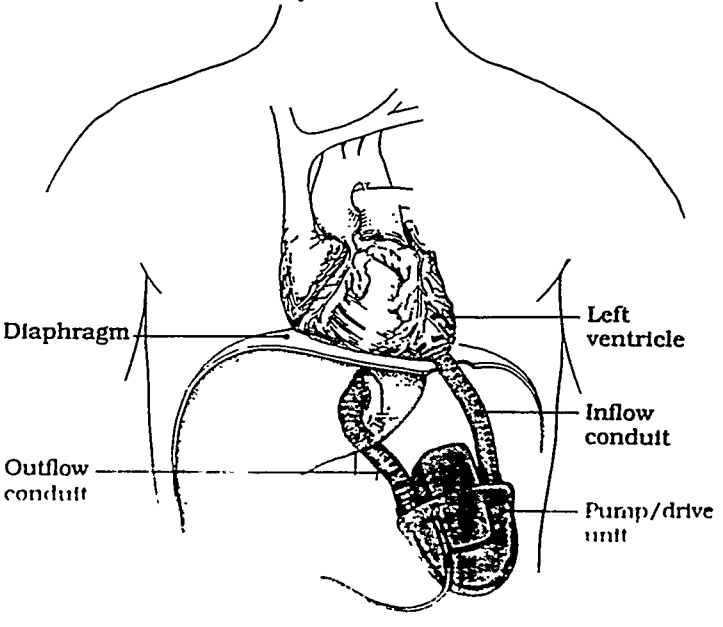

Figure 1. Anatomical configuration of the NLVAS.

2.0 APPROACH

To achieve such desired blood flow behavior, it is helpful, if not essential, to use advanced flow diagnostic tools. A commonly used flow diagnostic tool is laser doppler velocimetry (LDV). LDV provides an instantaneous measurement of velocities at a single point in a flow field. LDV systems are also well-developed and commercially available.

In the present effort, we are using LDV; however, the primary measurements are done with a technique called fluorescent image tracking velocimetry or FITV. FITV is a particle imaging velocimetry technique that enables measurements very close to biomaterial surfaces.

With advances in computer imaging equipment and pulsed lasers, applications of particle image velocimetry are increasing rapidly. Another reason for the popularity of particle imaging velocimetry is its simplicity: a fluid is seeded with particles that follow the fluid flow -- that is, neutrally-buoyant particles with low Stokes numbers and sizes much smaller than the length scales of the flow. A pulsed laser illuminates the seeded flow field at controlled intervals. The displacement of particles between laser pulses produces a velocity vector map of a flow field. From this, other important parameters, such as shear stress and particle residence time, are attainable.

Although the underlying concept of particle imaging velocimetry appears to be straightforward, considerable problems still remain. The main difficulties are in the acquisition of images with good signal-to-noise (S/N) ratios near flow boundaries and the digital analysis of images.

There are many variations of particle imaging velocimetry [7]. A double-pulse technique is known as particle image velocimetry or PIV. PIV produces a two-dimensional velocity map at an instant. The double-pulse technique has good spatial resolution but derives only the speed and orientation of velocity vectors — direction (sign) is unknown. A coded pulse sequence is one way to eliminate directional ambiguity. However, pulse coding often requires longer exposures and more pulses. This reduces spatial resolution due to the increased number and size of particle images. Yet another particle imaging velocimetry approach uses continuous pulsed illumination to produce Lagrangian trackings of particles through a flow field [8,9].

Refractive/reflective light scattering is adequate for most particle imaging applications. With enough illumination power, good signal-to-noise (S/N) ratios between particle images and the background are achievable. Near solid flow boundaries, however, the S/N ratio may diminish to the point that particle images are undetectable. This is because scattering (refractive/reflective scattering will simply be referred to as scattering) from solid flow boundaries is usually much stronger than from small particles. Even if the refractive indices of the fluid and flow boundary are matched, impurities in the solid flow boundary can still generate strong scattering.

Use of fluorescent particles and color filtering is one way to enhance S/N ratios near flow boundaries. Figure 2 illustrates the basic concept. A fluorescent-dyed particle is shown near a fluid-solid interface. A monochromatic light of wavelength λ_1 illuminates the scene.

When excited with light of an appropriate wavelength, the dye fluoresces or emits light. An important property of the fluorescent dye is its Stokes shift — the difference between excitation and emission wavelengths. Thus, the light from the particle shown in Figure 2 consists of both scattered light at the excitation wavelength (λ_1) and fluoresced light at a different wavelength (mean fluorescent emission, λ_2). The light scattered by the flow boundary in Figure 2 is at the same wavelength as the excitation light.

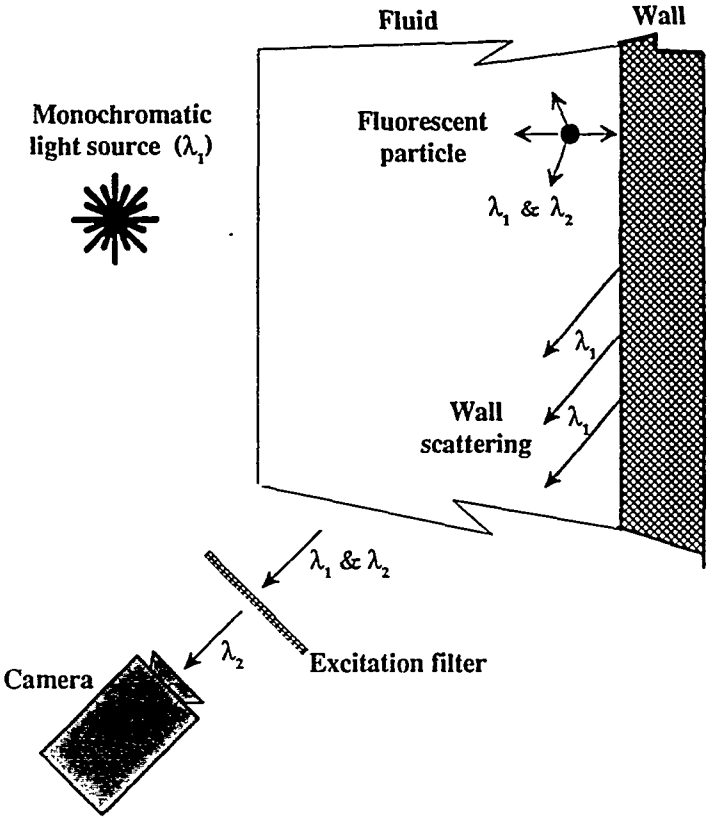

Figure 2. Illustration of fluorescent particle and color filtering concept for near-wall particle imaging

The S/N ratio is increased dramatically by placing an excitation filter in front of the camera. The excitation filter occludes the light scattered by the flow boundary and the particle at λ_1 — the camera sees only the fluorescent light emitted by particles at λ_2. This has provided excellent S/N ratios of particles close to biomaterial surfaces of the NLVAS.

3.0 EXPERIMENTAL SETUP

3.1 FITV SYSTEM

An FITV system consists of the following basic components: a pulsed excitation source, beam shaping optics, an excitation occlusion filter, an electronic camera with digital image acquisition system, and an image processing computer. Figure 3 shows the components of the USDOE's FITV system.

Excitation Light Sources The wavelength of the light source should be close to the peak excitation wavelength of the fluorescent dye. The excitation light source must produce pulsed light with accurate and controllable pulse timing. Continuous emission lasers with an acousto-optical modulator are ideal. Our experience indicates that at least 1 watt of optical power is necessary for FITV. See Adrian [7] and Shaffer et al. [8] for more information on pulsed light sources.

For this application, the excitation source is either an argon or a copper-vapor laser. The argon laser produces up to 5 watts of continuous light with the most powerful wavelengths (nm) at 488 (blue) and 514.5 (green). Other less powerful lines are present at wavelengths from 350 nm to 507.1 nm.

An electronically controlled acousto optic modulator (AOM) pulses the continuous beam of the argon laser. The AOM transmission rise time limits the AOM pulse capabilities. With a rise time of less than 50 ns, the AOM pulses can range from continuous transmission to repetition rates over 1 MHz and pulse durations less than a micro second.

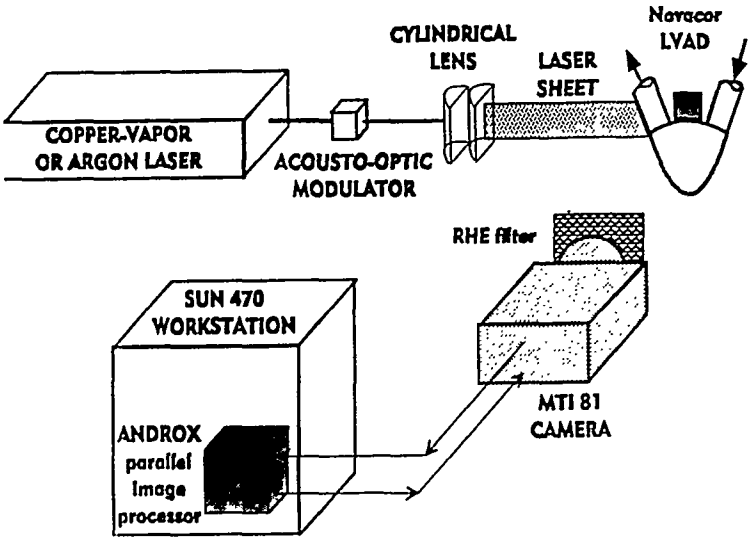

Figure 3. The USDOEs FITV system used for this application.

The copper-vapor laser is a pulsed laser with pulse durations of 30 ns and repetition rates up to 20 KHz. Pulse energies range from 0.5 to 2 mJ. It produces two primary wavelengths of 510.6 and 578.2 nm with a total average optical power of 10 W. Only the 510.6 nm wavelength is used for this application. The copper-vapor laser is used only if the required pulse durations become short enough that the pulse energies from the argon laser drop well below 0.5 mJ.

Beam shaping optics The beam shaping optics consist of a series of cylindrical lens [9,10]. They transform the circular cross section of the beam into a rectangular cross section with a large aspect ratio. This is commonly called a laser sheet.

Fluorescent-Dyed Particles Fluorescent particles are available from several commercial manufacturers. Some of the commercial manufacturers are Polyscience, [11], Duke Scientific [12], and Bangs laboratories [13]. Figure 4 shows the excitation and emission characteristics of a commercial fluorescent particle [12]. The dye in this particle is suitable for excitation with the green wavelengths of argon (514.5 nm) and copper-vapor (510.6 nm) lasers. Other fluorescent-dyed particles are available for excitation with lasers of different wavelengths.

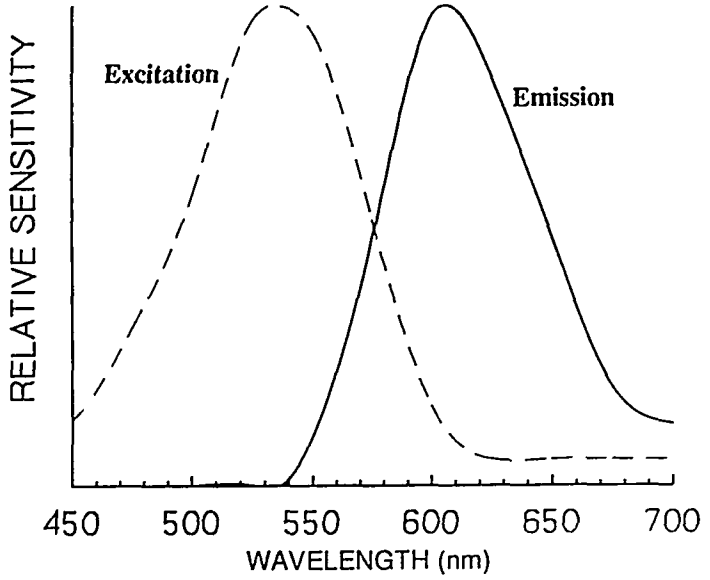

Figure 4. Excitation and emission spectra of a commercial fluorescent-dyed particle (Duke Scientific "red" fluorescent particles [12]).

Excitation Filters The purpose of the excitation filter is to occlude the excitation wavelength(s) and pass the fluorescent wavelengths. With monochromatic excitation, the ideal filter will block only a single wavelength. Three types of filters approach monochromatic occlusion: thin-film dielectric interference filters Raman holographic edge (RHE) filters, and colloidal Bragg diffraction filters. The mean occlusion characteristics of the interference and RHE filters are practically the same [14]. The transmission characteristics of an RHE [15] and a colloidal filter [16] are shown in Figure 5.

Since the Stokes shift is significant (>20 nm) for many fluorescent dyes, an edge filter can possibly be used. Edge filters are much less expensive than the notch filters. Figure 5 also shows the transmission curve of an inexpensive edge filter [17].

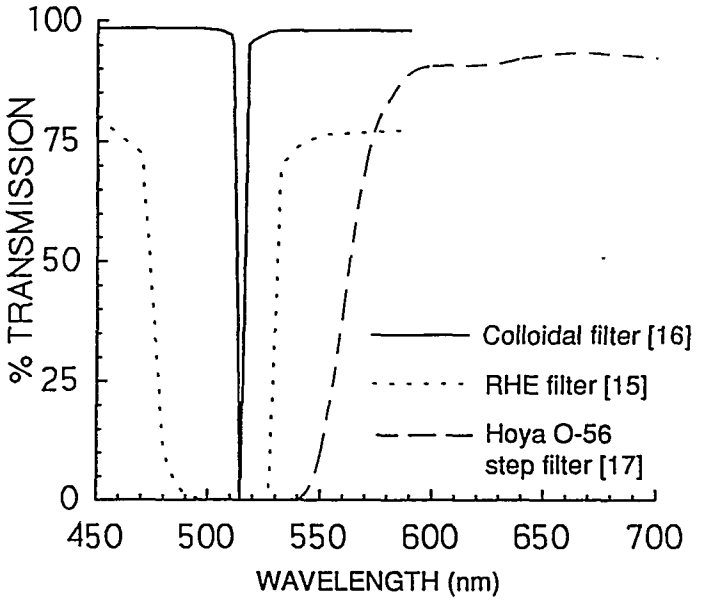

Figure 5. Example transmission spectra for notch and step filters.

Image acquisition system The camera is a MTI Model 81 tube camera. The camera scanning parameters are externally controlled through an ANDROX programmable video controller. An ANDROX analog-to-digital converter (ADC) digitizes the analog output of the MTI 81. With this setup, image resolutions from 512 x 512 pixels to 2048 x 1800 pixels are attained. The grey-level resolution of each pixel is 8 bits. The frame rate is variable from 10 frames per second (2048 x1800 pixel resolution) to 100 frames per second (512 x 512 pixel resolution).

Image processing computer system Processing and analysis of FITV images are done on a SUN 470 workstation equipped with an ANDROX parallel image processing subsystem. The ANDROX system accelerates many image processing functions by a factor of 50 or more over the SUN 470 CPU.

Over the past few years development of custom software to analyze PITV and FITV data has been underway at the DOE. The interested reader is referred references [18] and [19] for more information on this software.

3.2 CARDIAC SIMULATION FLOW LOOP

Figure 1 shows the Novacor LVAS in one of two anatomical configurations. The LVAS is placed extraperitoneally within the abdomen, with the inflow conduit connected to the left ventricular apex. The outflow conduit may be anastomosed to either the abdominal aorta (shown) or to the thoracic aorta. Because the LVAS receives its inflow from the left ventricle, inflow rates are highly variable, depending on the contractile status of the myocardium

In the immediate post-operative period, the contractility of the diseased myocardium is additionally depressed by anaesthetic agents. Under these conditions, the ventricle functions almost as a passive conduit and therefore the LVAS inflow is relatively constant. However, because the LVAS allows the myocardium to deliver flow at a greatly reduced afterload, myocardial contractile function may recover and increase beyond pre-implant values within a few days. The ventricle then acts as a "priming pump" for the LVAS, and the inflow to the LVAS becomes markedly pulsatile with peak flow rates of as much as four to five times greater than the immediate post-operative values.

For this study it is essential to acquire the FITV images under representative patient conditions, including varying degrees of myocardial contractility. For this purpose, an active mock loop has been designed (Figure 6). Inflow to the LVAS is provided by a servo-controlled piston pump which is able to produce an arbitrary flow waveform based on a voltage command. Using a programmable waveform generator, it is possible to generate LVAS inflow waveforms that accurately mimic inflows monitored from patients in the operating room or intensive-care unit at the University of Pittsburgh [20].

Flow patterns in the LVAS are also a function of the afterload presented to it. The LVAS afterload in this mock loop uses a calibrated compliance to simulate the systemic vascular compliance and a pneumatic pressure regulator to maintain the mean arterial pressure within physiological values independent of flow, just as occurs in the body via the baroreceptor reflex. The mock loop is instrumented with an ultrasonic transit-time flowmeter and clinical pressure transducers.

An NLVAS was manufactured from transparent materials to provide optical access for FITV. A transparent blood analog fluid which has a viscosity close to that of blood (4 cps) was also used. The blood analog fluid consists of a solution of 42% wt. aqueous spectrophotometric-grade glycerin.

The blood analog fluid was seeded with "red" fluorescent particles manufactured by Duke Scientific [12]. The particles consist of polystyrene latex and a proprietary mixture of fluorescent dyes. They are neutrally buoyant and their size is 30 ±2 micron.

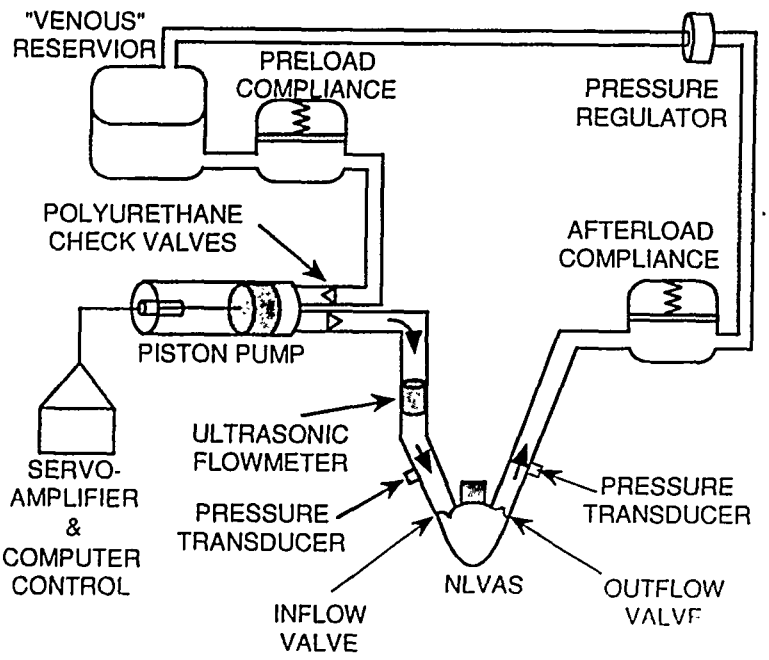

Figure 6. Cardiac simulation flow loop.

4.0 RESULTS

4.1 PERFORMANCE OF EXCITATION FILTERS

Several filters were tested for the present application. These include an RHE filter [15] and several inexpensive step filters. Rather than attempting an independent measurement of optical density, the performance parameter (S/N ratio) pertinent to this application was measured under typical operating conditions.

The test consisted of measuring the S/N ratios produced with our FITV system for a fixed, representative scene. The scene was a pericardial trileaflet valve in its transparent housing filled with blood analog fluid. The housing, pericardial valve, and blood analog fluid are the same as used in actual flow measurements. The only experimental variable was the type of excitation filter placed in front of the camera lens.

Figure 7 shows a pericardial valve used in the NLVAS. The valve is constructed of bovine heart tissue formed into three flexible leaflets that open and close to restrict flow to one direction. Figure 8 shows the pericardial valve in its transparent housing filled with blood analog fluid.

The valve leaflet material was found to have mild fluorescent properties. This is undesirable since it increases the background level. Dying the valve with a black clothing dye practically eliminates the valve's fluorescence.

In Figure 9, the same scene as in Figure 8 is illuminated with 1 W/cm^2 of 510.6 nm light from a copper-vapor laser. Figure 10 shows exactly the same scene as Figure 9 but with an RHE filter in front of the camera. Fluorescent particles are now noticeable. Some of the particles are suspended in the fluid while others are adhering to the surface of the pericardial valve or the walls of the transparent housing. The particles tended to move slowly due to radiative heating of the stagnant fluid by the laser light.

In Figure 10, the room lights are on so the valve and transparent housing are still visible. In Figure 11, the room lights are turned off so only the light emitted by the fluorescent particles is seen. Note that the fluorescent particles were also present in Figures 8 - 10.

As Figure 11 illustrates, the S/N ratio is excellent — even for particles adhering to the valve surface and housing walls. Both the RHE filter and Hoya O-56 filter produced S/N ratios exceeding the maximum level detectable with the FITV system used for this application.

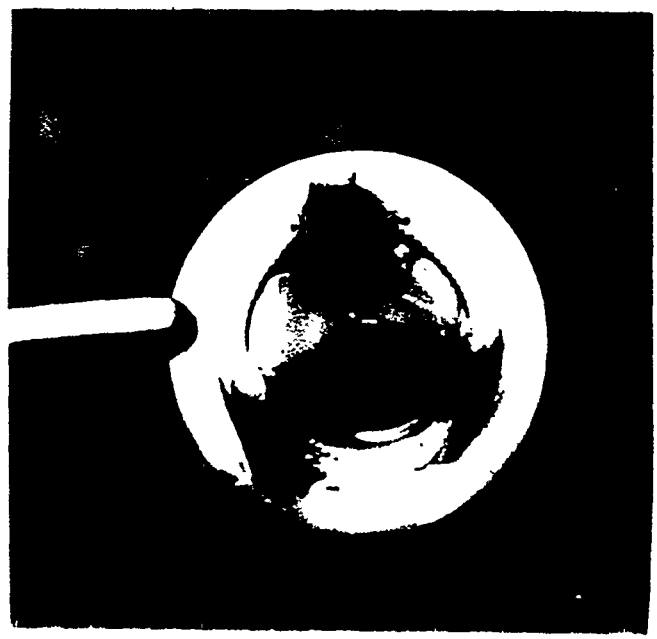

Figure 7 The pericardial trileaflet valve used in the NLVAD.

Figure 8. A pericardial valve in a transparent housing used for FITV measurements.

Figure 9. A copper-vapor laser illuminates the pericardial valve with 510.6 nm light.

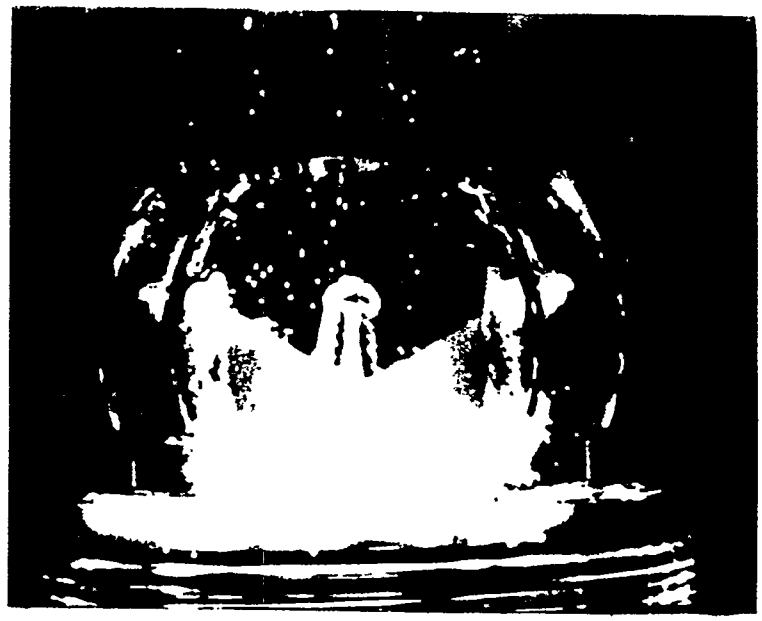

Figure 10. Same scene as in Figure 9, except an RHE filter is placed in front of the camera. Room lights are on so that valve and housing are visible.

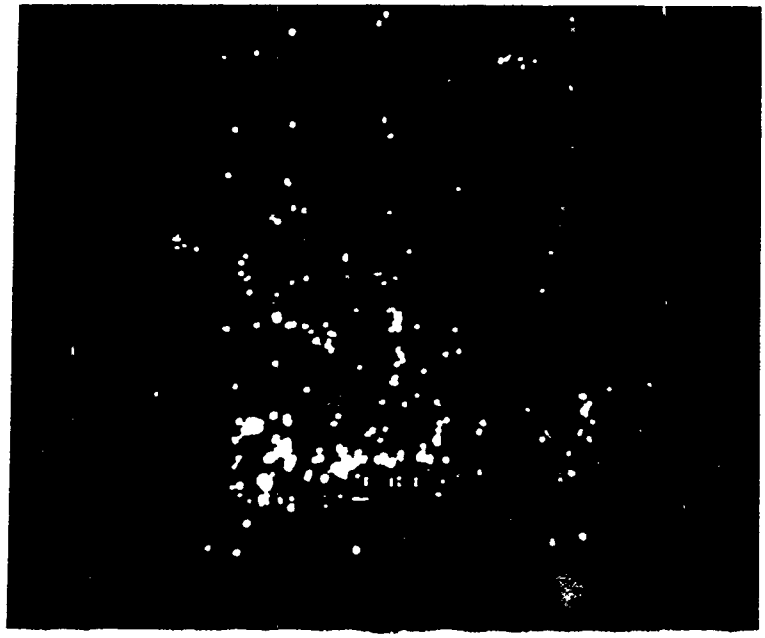

Figure 11. Same scene as Figure 10 but with room lights turned off.

4.2 EXAMPLE FITV MEASUREMENTS

The flow conditions for FITV measurements simulated the full range of clinical conditions observed for cardiac transplant patients at the University of Pittsburgh: pump rates ranged from 60 to 120 beats/minute with fill volumes ranging from 25 to 60 cc [20].

During a cardiac cycle, the FITV system acquires six images at fixed time separations. For example, if the cardiac cycle duration were 600 ms, six measurements are made at 100 ms separations. After digitizing six images into video-RAM, the images are compressed and stored on the SUN 470 hard disk. The acquisition and storage of six FITV images takes about 20 seconds. For a specific experimental condition, data is acquired for at least 100 cardiac cycles.

Figure 12 shows the location of one of the inflow pericardial valve flaps at 100 ms intervals through a 600 ms cardiac cycle. The images in Figure 12 are with constant room illumination and 50 ms exposure times. For the actual FITV measurements the room lights are off. The AOM delivers a sequence of pulses during each frame. For these initial measurements, the pulse sequence consists of four pulses at a fixed frequency. Software is under development at the DOF that will handle coded pulse sequences.

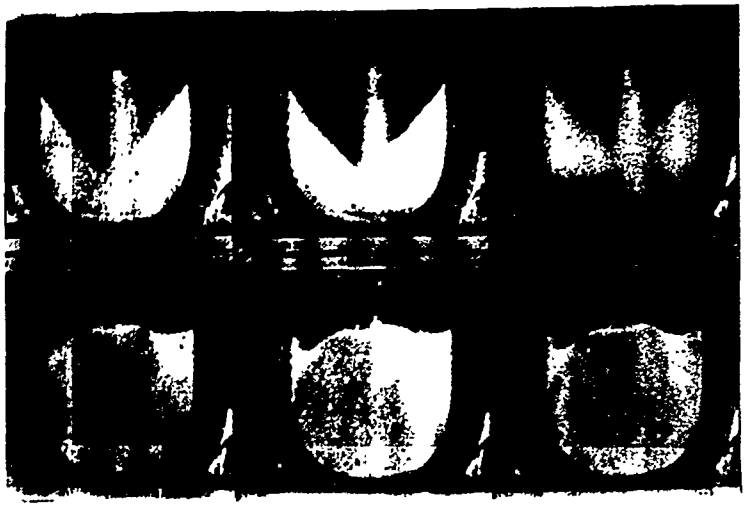

Figure 12. Location of the pericardial valve flaps (inflow)

Figure 13a and 13b show two examples of typical FITV images. Figure 13a is taken at the beginning of the systole (first frame of Figure 12); the flow velocities are high because valve flaps are in motion (closing). Figure 13b is taken near mid-diastole when the valve flaps are not moving (fully open) and the velocities are much lower. Consequently, to maintain reasonable spacings between consecutive particle images, the laser pulse frequency is varied from frame-to-frame throughout the cardiac cycle. For example, the pulse frequency in Figure 13a is 1 KHz and in Figure 13b it is 222 Hz.

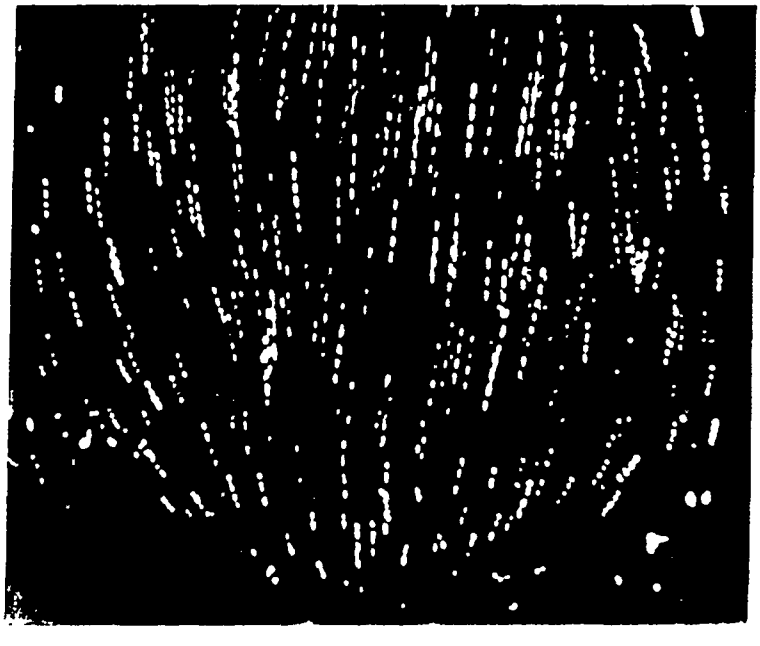

Figure 13a. Example FITV image taken 10 ms after the start of systole.

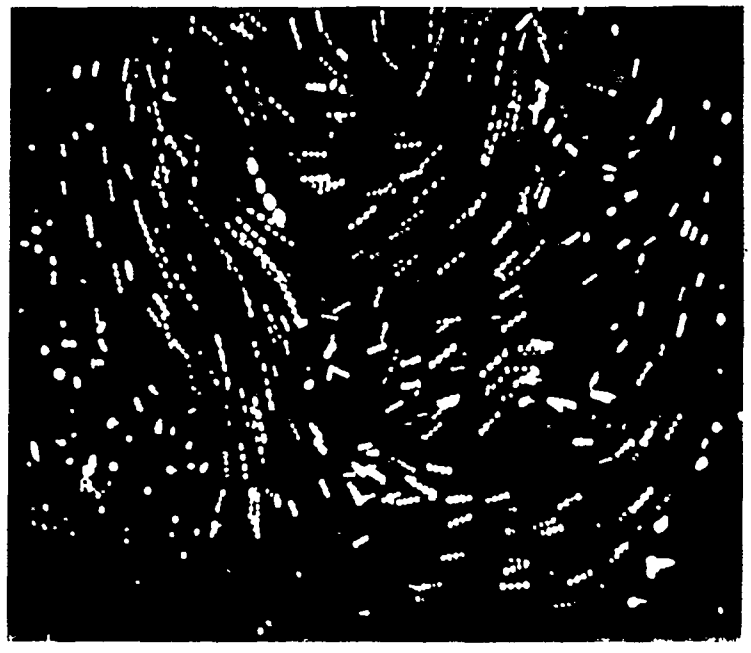

Figure 13b. Example FITV image near middle of diastole.

Figures 14a and 14b show initial attempts to visualize the FITV data extracted from Figure 13b. Figure 14a shows a contour map of velocity magnitude (speed). The brighter areas represent higher speeds and the darker areas lower speeds. Figure 14b shows a velocity vector map derived from Figure 13b. Arrowheads are not shown on the velocity vectors since, as explained earlier, uncoded pulse trains do not determine velocity direction (sign). An inverse-distance domain interpolation of the randomly located data of Figure 13b produces a uniform grid of property values. This was necessary to produce Figures 14a and 14b. Figures 14a and 14b are shown only as an example of the type of results produced by FITV measurements.

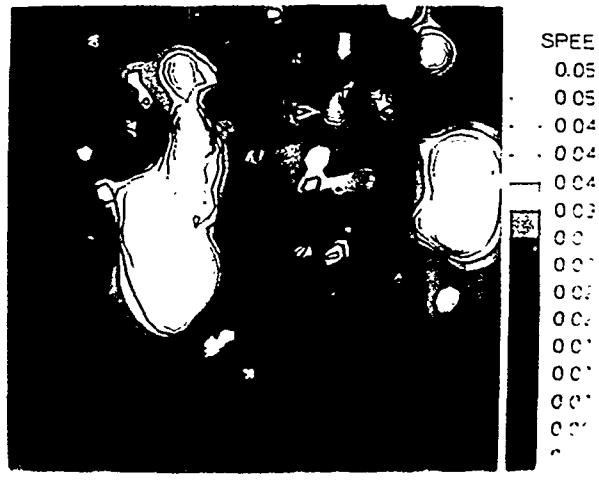

Figure 14a. A contour map of flow speed derived from FITV image shown in Figure 13b

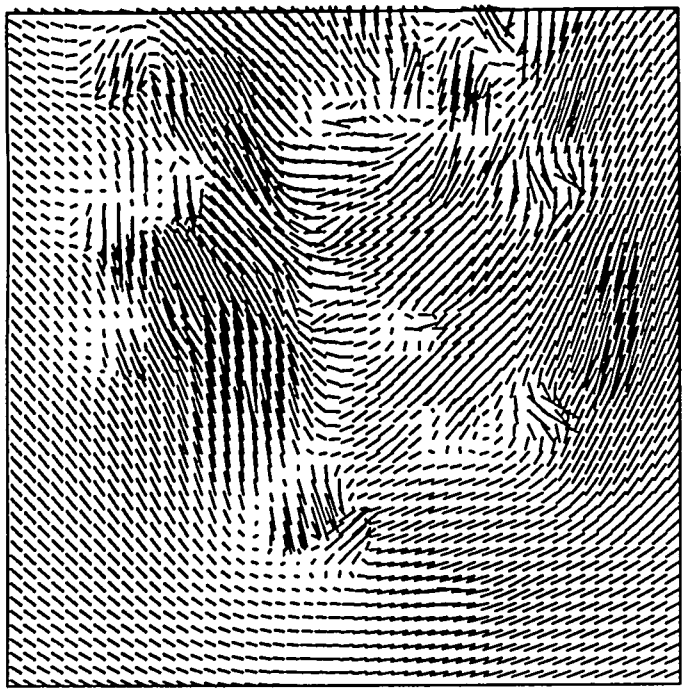

Figure 14b. A velocity vector map derived from FITV image shown in Figure 13b.

REFERENCES

[1] The Artificial Heart: Prototypes, Policies and Patients. edited by Hogness, J.R. and VanAntwerp, M., National Academy Press, Washington, DC, 1991.

[2] "Heart transplants: concerns about cost, access, and availability of donor organs," U.S. General Accounting Office Report to the Chairman, Subcommittee on Health, Committee on Ways and Means, House of Representatives, May, 1989.

[3] Poirier, V.L., "The Heartmate Cardiac Assist System," Cardiovascular Science & Technology: Basic and Applied, II, pp. 351, 1990-91.

[4] Portner, P.M., Oyer, P.E., Pennington, D.G., et al., "Implantable Electrical Left Ventricular Systems: Bridge to Transplantation and to the Future," Annals of Thoracic Surgery, Vol. 47, pp. 142-150, 1989.

[5] Kormos, R.L., Borovetz, H.S., Armitage, J.M. et al., "Evolving Experience with Mechanical Circulatory Support," Annals of Surgery, Vol, 214, pp. 471- 477, 1991.

[6] Didisheim, P., Olsen, D.B., Farrar, D.J. et al., "Infections and thromboembolism with implantable cardiovascular devices," Transactions of the American Society for Artificial Internal Organs, Vol. 35, pp. 54-70, 1989.

[7] Adrian, R.J., "Multi-point Optical Measurement of Simultaneous Vectors in Unsteady Flow - a Review," Int. J. Heat & Fluid Flow, Vol. 7, No. 2, June 1986.

[8] Shaffer, F.D., Ekmann, J.M, and Ramer, E.R., "Development of Pulsed Laser Velocimetry Systems with Photoelectric Image Sensors," AIAA Paper 88-3777, AIAA/ASME/ASCE/SIAM/APS First National Fluid Dynamics Congress, pp. 1944-1952, Cincinnati, Ohio, July 1988.

[9] Shaffer, F.D. and Ramer, E.R., "Pulsed Laser Imaging of Particle-Wall Collisions," Int. Conf. on Mechanics of Two-Phase Flow, Taipei, Taiwan, June 1989.

[10] Diemunsh, G. and Prenel, J.P., "A Compact Light Sheet Generator for Flow Visualization," Opt. Lasers, Vol. 19, No. 3, June 1987.

[11] Polyscience, Inc., Warrington, PA.

[12] Duke Scientific Corporation, Palo Alto, CA.

[13] Bangs Laboratories, Inc., Carnel, IN.

[14] Rich, C. and Cook, D., "Lippman Volume Holographic Filters for Rayleigh Line Rejection in Raman Spectroscopy," Physical Optics Corporation, Internal Report.

[15] Physical Optics Corporation, Torrance, CA.

[16] Flaugh, P.L., O'Donnel, S.E., and Asher, S.A., "Development of a New Optical Wavelength Rejection Filter: Demonstration of Its Utility in Raman Spectroscopy," Applied Spectroscopy, Vol. 38, No. 6, 1984.

[17] Hoya Optics, Inc., Freemont, CA.

[18] Ramer, E.R. and Shaffer, F.D., "Automated Analysis of Multiple-Pulse Particle Image Velocimetry Data," accepted for publication in the Journal of Applied Optics, 1991.

[19] Srinivasan, R., Singh, R., and Shaffer, F.D., "Image Analysis Techniques for Particle Tracking Velocimetry," submitted to the Int. Conf. on Pattern Recognition, Copenhagen, Denmark, 1992.

[20] Kormos, R.L., Borovetz, H.S., Pristas, J.M., et al., "LVAS pump performance following initiation of left ventricular assistance," Transactions of the American Society for Artificial Internal Organs, Vol. 36, pp. M703 M7705, 1990.